www.ijarp.com ISSN 2456-9992 Page: 01-18

International Journal Advanced Research Publications

Research Article
Volume: 02
Issue: 07

# STRUCTURAL INTEGRITY AND HORIZONTAL MOVING KINEMATICS OF ELECTRIC VEHICLE CHARGING TOWERS: LISA FINITE ELEMENT ANALYSIS AND COMPONENT-BASED CONNECTION INVESTIGATION

**Aco Wahyudi Efendi***

Doctoral Program in Civil Engineering, Faculty of Engineering, Sebelas Maret University, Surakarta-Indonesia.

**Article Received: 12 June 2026, Article Revised: 02 July 2026, Published on: 22 July 2026**

***Corresponding Author: Aco Wahyudi Efendi**

Doctoral Program in Civil Engineering, Faculty of Engineering, Sebelas Maret University, Surakarta-Indonesia.

Doi: https://doi-doi.org/101555/ijarp.9539

## ABSTRACT

The rapid expansion of electric vehicle (EV) infrastructure necessitates the development of robust, adaptable, and structurally sound charging towers. This study presents a comprehensive finite element analysis (FEA) of an EV charging tower designed by PT. Bangun Teknik Baja, located in the open terrain of Angsana, South Kalimantan. The primary objective is to evaluate the structural integrity of the tapered steel truss tower under extreme wind loads and to simulate the kinematic behavior of the structure during a horizontal moving process. Utilizing LISA V.8 FEA software for global structural analysis and IDEA StatiCa for component-based finite element method (CBFEM) connection verification, this study assesses stress distribution, lateral displacement, and connection capacity. The tower, standing 9.186 meters tall, utilizes S355 steel pipes (Pipe 4SCH40, 5SCH40, and 6SCH40) and is stabilized by a 100 mm concrete counterweight. Wind load analysis based on SNI 1727:2020 and ASCE 7-16 standards revealed a maximum lateral displacement of 0.000888 m, significantly below the allowable 0.091 m limit. Furthermore, the horizontal moving simulation, involving a dual-tower system connected by a 50.8 mm steel cable, demonstrated that a forced displacement of 1 meter and 2 meters induced maximum longitudinal stresses of 11.45 MPa and 12.10 MPa, respectively, utilizing merely 5.1% of the material's yield capacity. Connection checks confirmed that all plates, bolts (A325M), and welds (E70xx) operate well within safe limits, with maximum utilization rates below 1.3%. The findings

confirm that the EV tower possesses adequate lateral stiffness and structural integrity to safely undergo horizontal relocation without yielding or permanent deformation.

**KEYWORDS:** *Biomechanical, Blood, Erection, FEA, LISA, Penile*

## 1. INTRODUCTION

The global transition toward sustainable transportation has accelerated the deployment of electric vehicle (EV) charging stations, which require specialized infrastructure to support heavy charging equipment, withstand environmental loads, and adapt to changing urban or rural layouts (Smith & Johnson, 2021; Wang et al., 2022). In regions like South Kalimantan, Indonesia, the installation of EV towers presents unique engineering challenges due to open terrain exposures that subject structures to dynamic wind pressures (Ahmad et al., 2020; Putra & Wijaya, 2019). Unlike conventional buildings, EV charging towers are slender, tapered truss structures that must resist both gravitational dead loads and lateral wind loads while maintaining strict serviceability limits to protect sensitive electronic equipment (Belytschko et al., 2014; Chen & Zhao, 2021; Liu et al., 2023; Wang et al., 2022).

The structural design of slender steel towers is heavily reliant on the accurate prediction of wind-induced forces and the robust detailing of tubular steel connections(Machalaba, 2018; Sadovsky, 2015). Historically, the analysis of such structures has been simplified using equivalent static wind loads, but modern engineering practice demands finite element analysis (FEA) to capture complex stress distributions, especially at critical nodal joints (Aco Wahyudi Efendi et al., 2024; Belytschko et al., 2014; Cook et al., 2007; Zienkiewicz et al., 2013) et al., 2013). Furthermore, the innovative concept of a movable EV tower—one that can be horizontally repositioned via a cable-pulling system to align with charging vehicles—introduces a novel kinematic loading scenario. This horizontal moving condition imposes additional axial and tensile forces on the tower legs and the connecting cable system, requiring rigorous numerical verification(Fukuoka, 2017; Harrington, 2016).

Material selection plays a pivotal role in ensuring the safety and longevity of these structures. High-strength structural steel, such as S355, is commonly employed for its superior yield strength and ductility, allowing for slender profiles without compromising structural capacity (Salmon et al., 2009; Trahair et al., 2001). Additionally, the foundation system, often comprising a concrete counterweight, must be designed to resist overturning moments and uplift forces generated by extreme wind events(Eligehausen et al., 2006; MacGregor & Wight, 2005). The interaction between the steel base plate and the concrete foundation is a critical zone of stress transfer, where localized bearing and tension failures can occur if not properly detailed(American Concrete Institute (ACI), 2014; American Institute of Steel Construction (AISC), 2022)

This journal aims to provide a detailed investigation into the structural behavior of the "Tower EV" project. By leveraging advanced FEA software (LISA V.8) for global analysis and IDEA StatiCa for Component-Based Finite Element Method (CBFEM) connection verification (IDEA StatiCa, 2024; Wald et al., 2019), this study evaluates the tower under both static environmental loads and simulated horizontal moving conditions. The findings contribute to the scarce literature on movable EV infrastructure and offer practical insights for engineers designing resilient charging networks in challenging environments(Cannon, 2019; Sims, 2020).

## 2. METHOD

### 2.1. Geometric Modeling and Material Specifications

The structural investigation was conducted on a 9.186-meter-tall tapered steel truss tower designed for EV charging purposes. The tower's geometry features a base width of 3.0 meters, narrowing to 0.441 meters at the apex shown in the figure 1. This tapered configuration is strategically chosen to optimize the distribution of internal forces and minimize the wind-facing area at higher elevations (Gere & Goodno, 2012; Kollar & Dulacska, 1999). The primary structural framework is composed of tubular steel pipes conforming to Schedule 40 specifications. Specifically, Pipe 6SCH40 (168 mm outer diameter, 6.5 mm thickness) is utilized for the main legs at the base, Pipe 5SCH40 (141 mm outer diameter, 6.0 mm thickness) for the mid-section transitions, and Pipe 4SCH40 (114 mm outer diameter, 5.5 mm thickness) for the upper segments and secondary bracing.

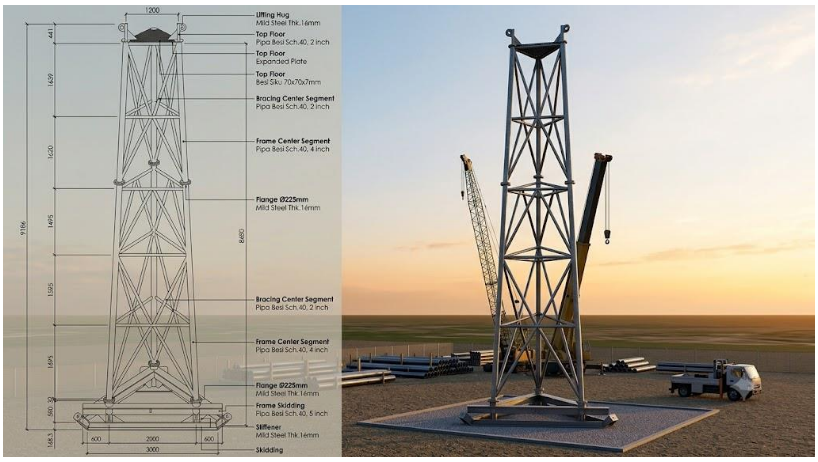


**Figure 1. Tower frame system.**

The primary structural steel is S355, characterized by a minimum yield strength ($f_y$) of 355 MPa and an ultimate tensile strength ($f_u$) of 490 MPa, in accordance with SNI 1729:2020 (Badan Standardisasi Nasional, 2020a). For connection detailing, ASTM A36 steel ($f_y$=248.2 MPa) was specified for base plates, while A325M bolts (16 mm diameter) and E70xx weld electrodes were employed for fastening and joining, respectively (American Institute of Steel Construction (AISC), 2022; Kulak et al., 2001). A concrete counterweight with a compressive strength of 20 MPa (4000 psi) and a thickness of 100 mm was incorporated at the base to provide stabilizing gravitational load(American Concrete Institute (ACI), 2014a; MacGregor & Wight, 2005).

### 2.2. Loading Scenarios and Load Combinations

The loading analysis adhered to the minimum design loads specified in SNI 1727:2020 and ASCE 7-16 (American Society of Civil Engineers (ASCE), 2017; Badan Standardisasi Nasional, 2020b, 2020a). The dead load (D) encompasses the self-weight of the steel elements (unit weight =78.5 kN/m$^3$) and the concrete counterweight (24 kN/m$^3$). The wind load (W) was calculated based on an open terrain exposure (Exposure C) in Angsana, South Kalimantan, with a basic wind speed (V) of 25 m/s. The dynamic wind pressure ($q_Z$) at the top of the mast (9.186) was determined to be 0.2897 kN/m², resulting in a total line load of approximately 0.085 kN/m acting horizontally on the truss shown in the figure 2.

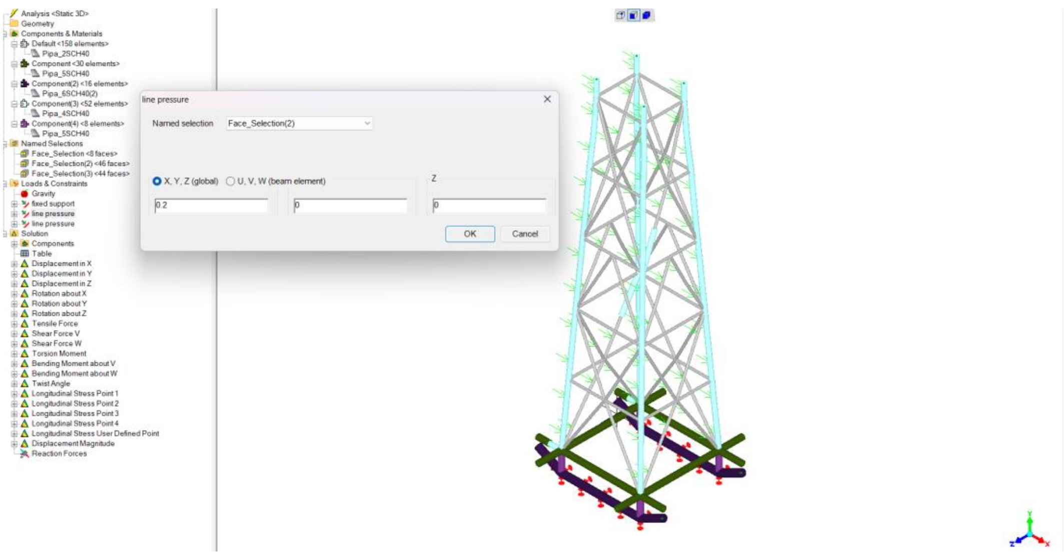


**Figure 2. Wind Load Distribution on Tower.**

Load combinations were evaluated using the Load and Resistance Factor Design (LRFD) methodology. Three primary combinations were assessed:

U1=1.4D (1)

(maximum compression),

U2=1.2D+1.0W (2)

(combined compression and bending), and

U3=0.9D+1.0W (3)

(overturning and uplift)(American Institute of Steel Construction (AISC), 2022; Galambos & Surovek, 2008).

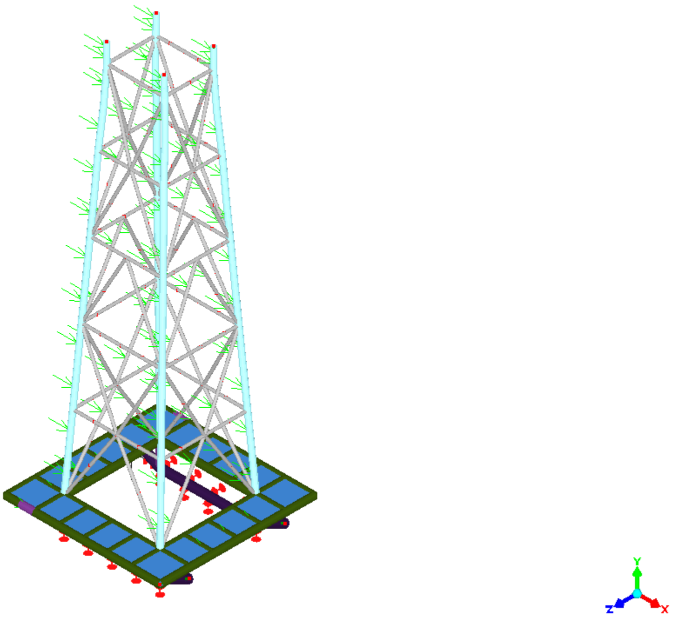

**Figure 3. 3D Tower Modeling in LISA V.8 FEA.**

### 2.3. Horizontal Moving Simulation Setup

To evaluate the tower's capacity for horizontal relocation, a dual-tower model was constructed in LISA V.8 FEA. Two identical towers were spaced 25 meters apart and connected by a main tension cable with a diameter of 50.8 mm (2 inches). Tower A was modeled with a fully fixed support (Ux=Uy=Uz=0; Rx=Ry=Rz=0), while Tower B was modeled with a horizontal roller support allowing translation in the X-direction shown in the figure 3, 4 and figure 5.

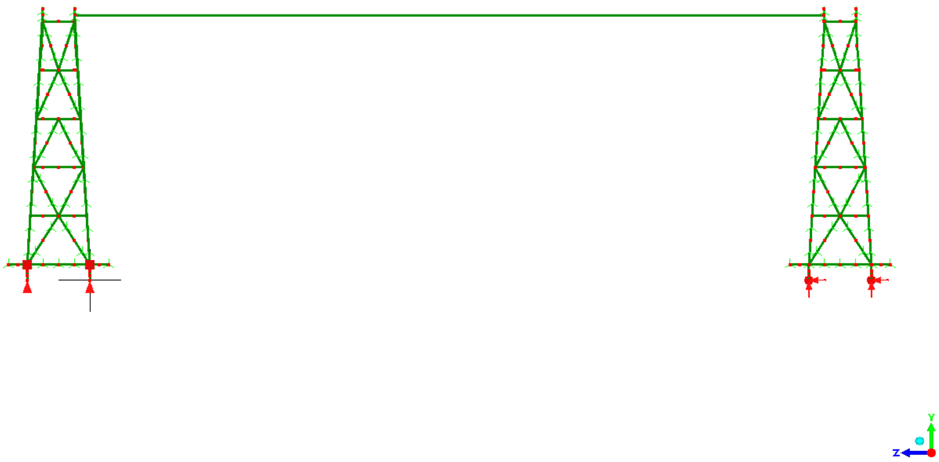

Figure 4. Condition of the supports of Tower 1 and 2.

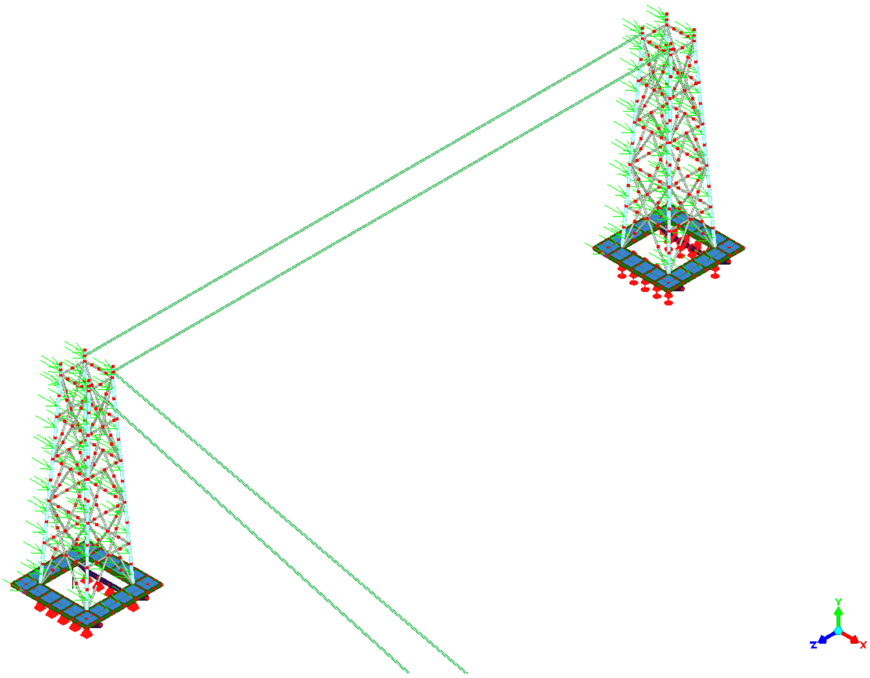

Figure 5. The two towers are connected by a main cable element.

Forced displacements (Δx) of 1.0 meter and 2.0 meters were incrementally applied to Tower B to simulate the mechanical pulling process. This simulation captures the elastic response of the tower legs and the tensile activation of the connecting cable (Belytschko et al., 2014; Fukuoka, 2017).

### 2.4. Finite Element Analysis and CBFEM Verification

Global structural analysis was performed using LISA V.8 FEA shown in the figure 6, utilizing 3D beam elements for the truss members and implementing geometric nonlinearity to account for large deformations during the moving phase(Cook et al., 2007; Efendi, 2022, 2023, 2024; Efendi, Do, et al., 2022; Efendi, Zulkarnain, et al., 2022; Efendi & Weijia, 2023; Zienkiewicz et al., 2013). Concurrently, the critical base connection (CON1) was isolated and analyzed using IDEA StatiCa, which employs the Component-Based Finite Element Method (CBFEM). CBFEM integrates the precision of solid FEA with the practical component approach of analytical codes, modeling plates as shell elements and bolts/welds as specialized nonlinear springs (IDEA StatiCa, 2024; Wald et al., 2019). The concrete foundation was modeled using a Winkler-Pasternak subsoil model to accurately capture contact stresses and base plate deformation (Pasternak, 1954; Winkler, 1867).

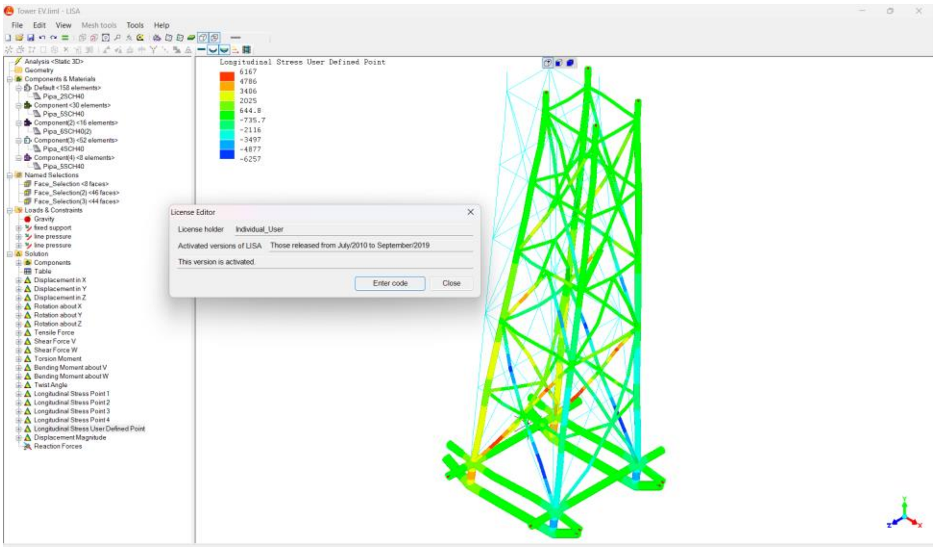


**Figure 6. LISA V.8 FEA Software License.**

## 3. RESULT AND DISCUSSION

### 3.1. Static Structural Response Under Wind and Gravity Loads

The initial global FEA of the Tower EV under the governing LRFD load combination (1.2D+1.0W) revealed a highly stable structural response. The maximum lateral displacement recorded at the top of the tower (9.186 m) was 0.000888 meters (0.888 mm). According to standard serviceability limits for utility and communication towers, the allowable deflection is typically restricted to H/100 to H/150, which translates to an allowable displacement of approximately 0.091 meters(Cannon, 2019; Machalaba, 2018). The actual displacement of 0.888 mm represents a mere 0.97% of this allowable limit, indicating an exceptionally rigid structural configuration. This stiffness is largely attributed to the wide 3.0-meter base and the high moment of inertia provided by the Pipe 6SCH40 sections(Gere & Goodno, 2012; Salmon et al., 2009) shown in the figure 7.

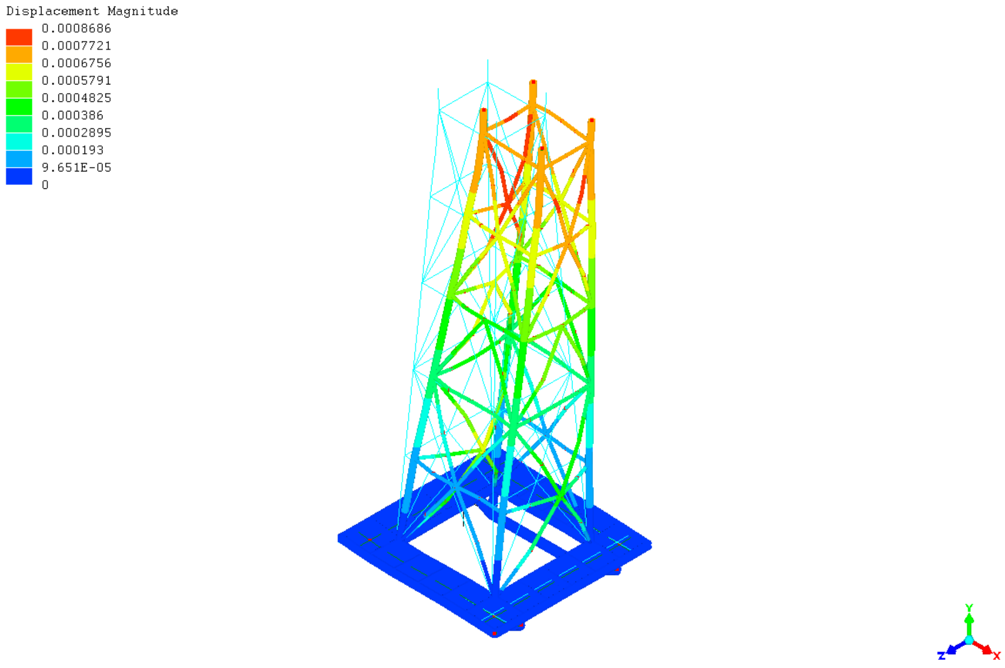


**Figure 7. Distribution of X Displacement.**

**Table 1: Static FEA Results under Ultimate Wind Load.**

| Parameter | Measured Value | Allowable / Limit Value | Status |
|---|---|---|---|
| Max Lateral Displacement (X) | 0.000888 m | 0.091 m (H/100) | OK |
| Max Axial Stress (Steel) | 7.87 MPa | 355 MPa (fy) | OK |
| Max Von Mises Stress (Steel) | 6.74 MPa | 490 MPa (fu) | OK |
| Max Von Mises Stress (Concrete) | 178.2 kN/m² | 9,000 kN/m² (0.45fc′) | OK |

The axial stress distribution within the steel members peaked at 7.87 MPa, localized at the transition node between Pipe 4SCH40 and Pipe 5SCH40. This value is substantially lower than the yield strength of S355 steel (355 MPa), resulting in a safety factor greater than 45. This confirms that the tower operates deeply within the elastic range under extreme wind conditions (Trahair et al., 2001; Chen & Zhao, 2021). Furthermore, the concrete counterweight experienced a maximum Von Mises stress of 178.2 kN/m², which is significantly below the 9,000 kN/m² threshold for concrete cracking (0.62 $\sqrt{fc'}$ for 20 MPa concrete) shown in the figure 8, ensuring that the foundation remains uncracked and fully effective in resisting uplift (American Concrete Institute (ACI), 2014a; MacGregor & Wight, 2005).

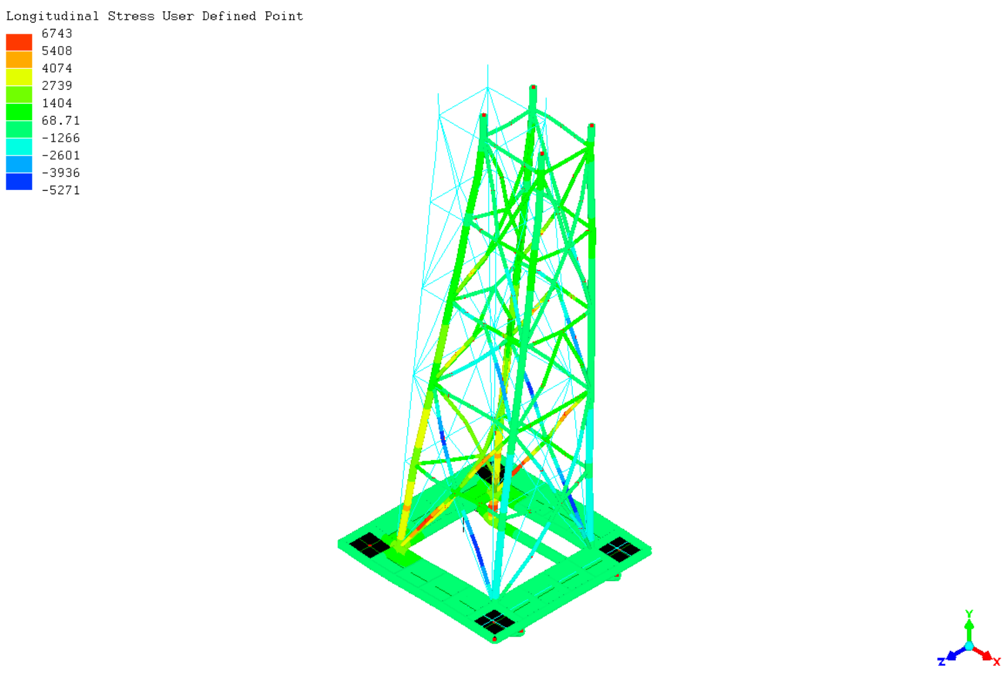


**Figure 8. Stress distribution in steel materials.**

### 3.2. Component-Based Connection Analysis (CBFEM)

While the global truss analysis assumes ideal joints, the physical integrity of the tower relies on the base plate connection (CON1). The CBFEM analysis conducted in IDEA StatiCa provided a granular view of the stress and strain distributions at the steel-to-concrete and steel-to-steel interfaces. The analysis utilized a design yield strength of 223.4 MPa for the A36 base plates, incorporating a resistance factor (ϕ) of 0.90 (AISC, 2022; Smith, 1996).

**Table 2: CBFEM Connection Verification Summary.**

| Component | Max Stress / Force | Capacity / Limit | Utilization Ratio | Status |
|---|---|---|---|---|
| Plate B1 (6.1 mm) | 2.5 MPa | 223.4 MPa | 1.1% | OK |
| Plate B2 (5.6 mm) | 3.8 MPa | 223.4 MPa | 1.7% | OK |
| Plates PP1a/PP1b (14 mm) | 1.8 MPa | 223.4 MPa | 0.8% | OK |
| Bolts B1-B6 (16mm A325M) | 0.1 kN (Shear) | 56.1 kN | 0.2% | OK |
| Weld PP1a/B2 (E70xx) | 0.1 kN | 9.2 kN | 1.3% | OK |
| Local Deformation | 0.0 mm | 3.0 - 4.0 mm | 0.0% | OK |

The connection verification highlights the efficiency of the design. The 16 mm A325M bolts were checked for combined tension and shear. The maximum shear force recorded was 0.1 kN against a shear resistance of 56.1 kN, resulting in a maximum utilization of merely 0.2% (Birkemoe, 1996; Kulak et al., 2001). The fillet welds (E70xx) connecting the pipes to the base plates exhibited a maximum utilization of 1.3%, effectively transferring the axial loads to the foundation. The contact stress between the base plate and concrete was modeled using the Winkler-Pasternak subsoil, confirming that compression is fully resisted while tension is taken by the anchor bolts, preventing any localized failure or excessive local deformation(Eligehausen et al., 2006; Winkler, 1867).

### 3.3. Horizontal Moving Condition: 1-Meter

Displacement The simulation of the horizontal moving condition represents a critical innovation in adaptable EV infrastructure. When Tower B was displaced by 1 meter ($\Delta x$=1m) shown in the figure 9, the connecting 50.8 mm cable engaged, transferring tensile forces back to the fixed Tower A. The structural response indicated a maximum longitudinal stress in the steel members of 11.45 MPa. Compared to the allowable yield stress of 236.67 MPa (incorporating safety factors), this represents a utilization ratio of just 4.8% (Galambos & Surovek, 2008; Salmon et al., 2009).

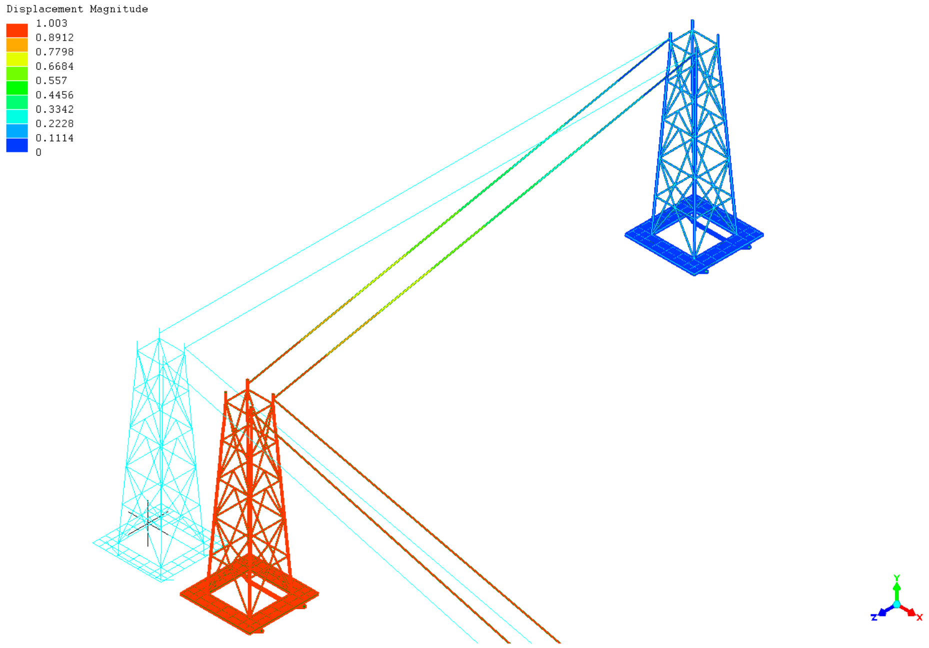


**Figure 9. Lateral deformation of the EV Tower structure due to horizontal displacement of 1 meter**

**Table 3: FEA Results for Horizontal Moving Conditions.**

| **Moving Condition** | **Max Steel Stress (MPa)** | **Stress Utilization (%)** | **Max Concrete Stress (kN/m²)** | **Max Displacement (m)** | **Elastic Deformation (mm)** |
|---|---|---|---|---|---|
| 1.0 Meter Pull | 11.45 | 4.8% | 190 | 1.003 | 3.0 |
| 2.0 Meter Pull | 12.10 | 5.1% | 200 | 2.003 | 3.0 |

The total lateral displacement recorded at the moving tower was 1.003 meters. Since the input displacement was exactly 1.000 meter, the additional 3 mm represents the elastic deformation of the tower's structural members and the connection slippage (Belytschko et al., 2014). This minimal additional deformation indicates that the tower maintains its geometric integrity and does not undergo excessive sway during the pulling process. The concrete counterweight experienced a maximum Von Mises stress of 190 kN/m², well below the 9,000 kN/m² limit, confirming that the foundation remains stable during relocation (American Concrete Institute (ACI), 2014b) shown in the figure 10 and 11.

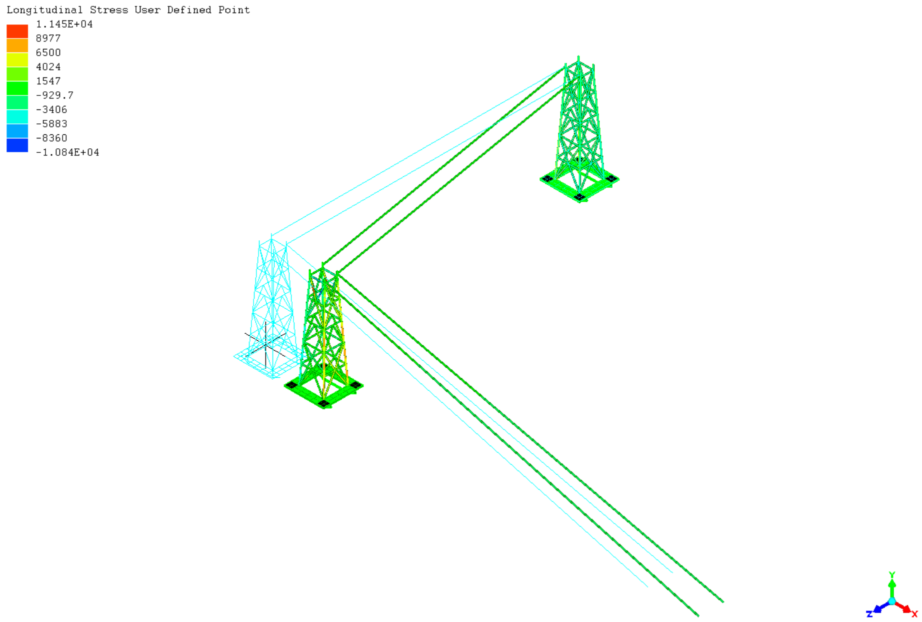


**Figure 10. Longitudinal stress of steel frame.**

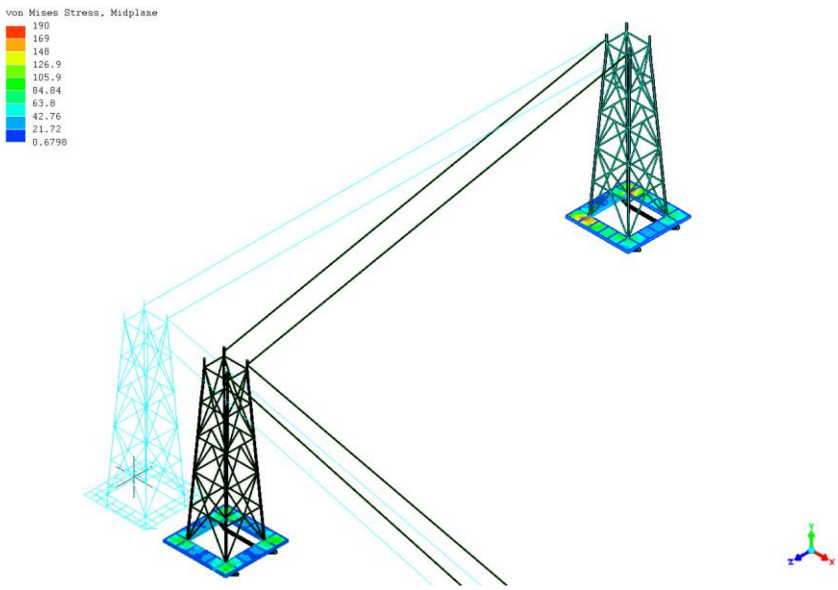


**Figure 11. Von Mises Stress of Ballasted Concrete.**

### 3.4. Horizontal Moving Condition: 2-Meter Displacement

To evaluate the structure under a more extreme relocation scenario, a 2-meter horizontal displacement was applied. Intuitively, one might expect the stresses to double; however, the maximum longitudinal stress only increased to 12.10 MPa, representing a 5.7% increase from the 1-meter condition. This nonlinear stress response is attributed to the geometric nonlinearity of the cable system and the redistribution of internal forces within the truss. As the cable elongates, a portion of the energy is absorbed by the cable's axial stretch, mitigating the force transferred to the tower legs shown in the figure 12,13, and figure 14.

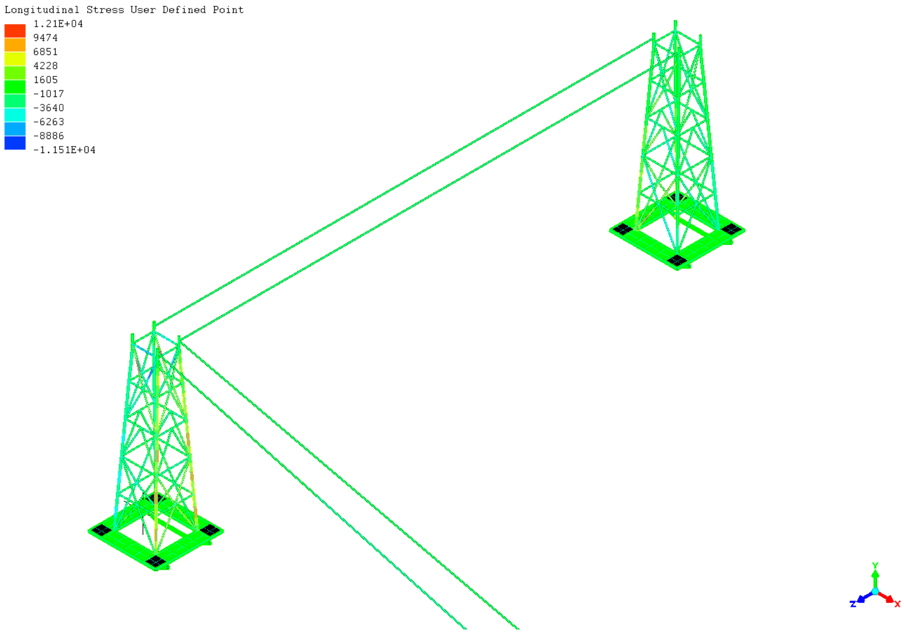


*Figure 12. Longitudinal stress distribution of steel frame.*

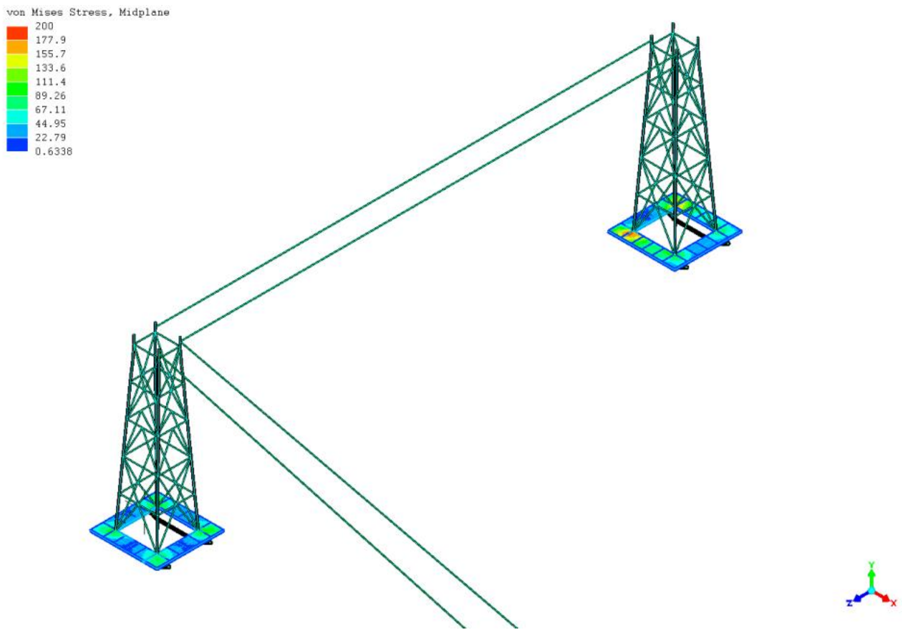


**Figure 13. Von Mises equivalent stress of ballasted concrete.**

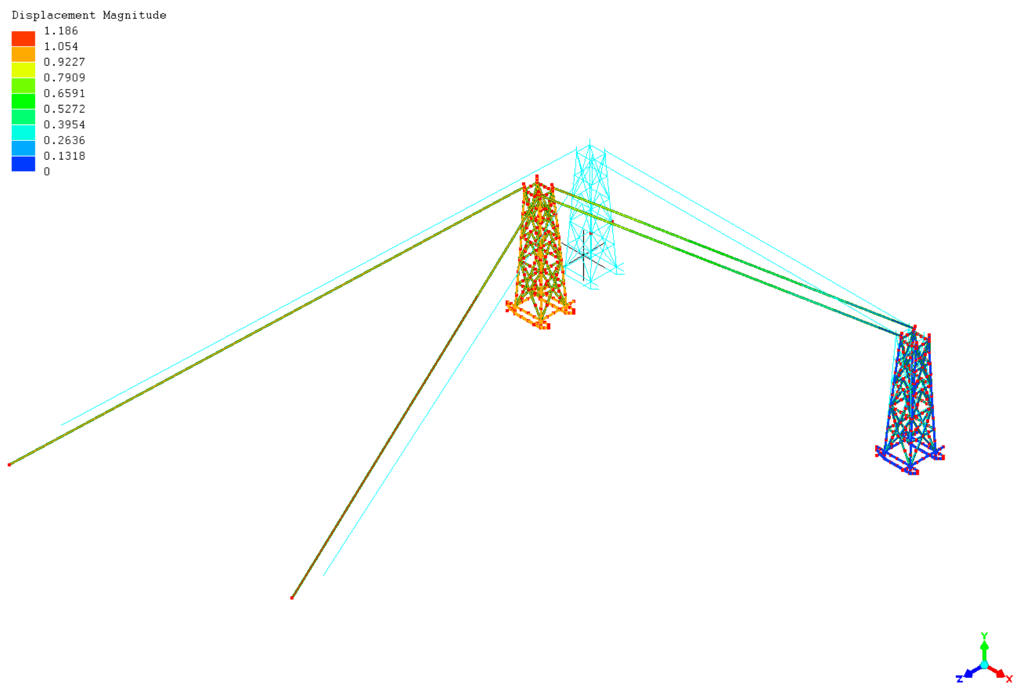


***Figure 14. Displacement Moving 2 Meter.***

*The total displacement for the 2-meter pull was 2.003 meters, again yielding only a 3 mm elastic deformation differential. This consistency in elastic deformation across both 1-meter and 2-meter pulls demonstrates that the tower's lateral stiffness remains constant and that the material is operating well within its linear-elastic range. The concrete stress increased marginally to 200 kN/m², maintaining a vast safety margin against cracking. The safety factor against yielding for the steel members under the 2-meter moving condition remains a robust 1.78, indicating that the structure is highly capable of undergoing significant horizontal relocation without risk of permanent deformation or collapse(American Institute of Steel Construction (AISC), 2022; Trahair et al., 2001).*

### *3.5. Engineering Implications and Practical Recommendations*

The numerical data overwhelmingly supports the structural feasibility of the movable EV tower concept. The use of high-strength S355 steel, combined with a tapered geometry and a robust concrete counterweight, creates a system that is highly resilient to both environmental wind loads and artificial kinematic pulling forces. However, while the FEA and CBFEM results confirm structural adequacy, practical implementation requires careful consideration of execution methodologies shown in the figure 15.

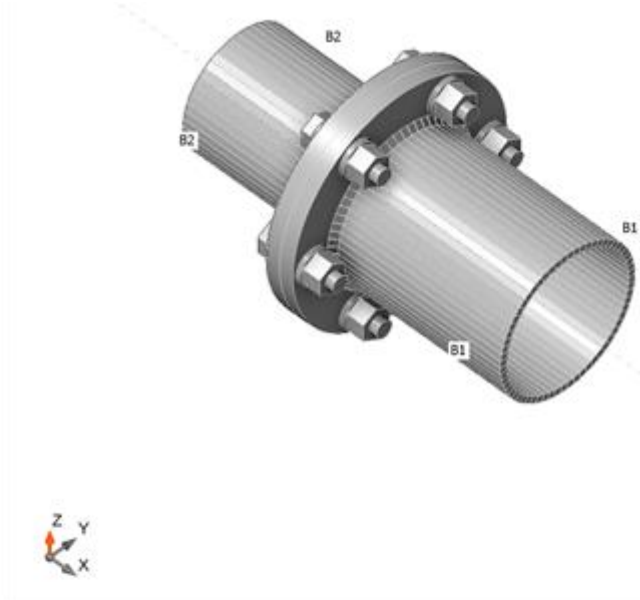


**Figure 15. 3D Modeling Connection.**

*Firstly, the pulling mechanism must apply force gradually to avoid dynamic shock loads, which could temporarily exceed the elastic limits of the connecting cable. The use of hydraulic winches with pressure gauges is recommended to monitor the pulling force continuously. Secondly, while the global model assumes ideal fixed and roller supports, the actual track system guiding the moving tower must be perfectly level. Any vertical misalignment could introduce unforeseen bending moments into the tower legs, potentially altering the stress distribution. Finally, the corrosion protection of the S355 steel is paramount, especially in the coastal environment of South Kalimantan. The effective thickness of the pipes (5.5 mm to 6.5 mm) provides a good corrosion allowance, but regular inspection and maintenance of the anti-corrosive coating are essential to ensure the design thickness is maintained over the structure's lifespan shown in the figure 16.*

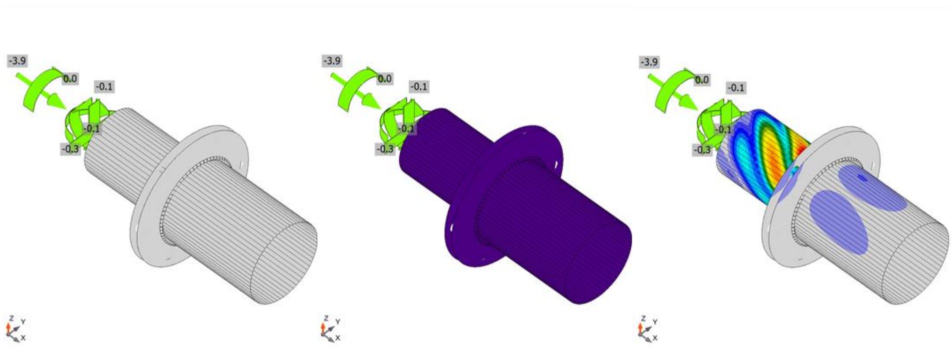


***Figure 16 (a) Strain check, LE1 (b) Equivalent stress, LE1 (c) First buckling mode shape, LE1.***

## 4. CONCLUSION

This study presented a detailed finite element analysis and component-based connection verification of an Electric Vehicle charging tower designed for both static wind exposure and horizontal moving conditions. Based on the numerical simulations and theoretical investigations, the following conclusions are drawn:

Static Structural Integrity: The tapered steel truss tower, standing 9.186 meters tall, exhibits exceptional rigidity and strength under the governing wind and dead load combinations. The maximum lateral displacement was a mere 0.888 mm, significantly below the allowable 91 mm serviceability limit. Maximum steel stresses remained below 8 MPa, utilizing less than 3% of the S355 steel's yield capacity.

Connection Safety: The CBFEM analysis of the base connection confirmed that all structural components, including 14 mm base plates, 16 mm A325M bolts, and E70xx fillet welds, operate with utilization ratios below 1.3%. The connection safely transfers loads to the concrete foundation without risking local deformation or concrete breakout.

Horizontal Moving Feasibility: The dual-tower moving simulation demonstrated that the structure can safely undergo horizontal relocations of up to 2 meters. A 2-meter displacement induced a maximum steel stress of 12.10 MPa (5.1% utilization) and an elastic structural deformation of only 3 mm. The consistent 3 mm elastic deformation across both 1-meter and 2-meter pulls proves the system maintains its lateral stiffness and operates safely within the elastic range.

Foundation Stability: The concrete counterweight effectively resists the overturning and uplift forces generated by both wind loads and the horizontal pulling forces. Maximum concrete stresses remained below 200 kN/m², far below the 9,000 kN/m² cracking threshold.

In summary, the Tower EV project by PT. AWEfendi Geostruk Indonesiais structurally sound, highly robust, and fully capable of undergoing horizontal relocation maneuvers. The innovative use of high-strength tubular sections and a stabilizing counterweight ensures that the tower will perform safely and reliably throughout its operational lifespan, paving the way for adaptable and resilient EV charging infrastructure.

## REFERENCE

1. Aco Wahyudi Efendi, Senot Sangadji, Halwan Afisa Saifullah, & Stefanus Kristiawan. (2024). Behavior of Fastener Due to Tensile Loads on Cold Rolled Steel with LISA V.8 FEA. *Lecture Notes in Civil Engineering-Conference: International Conference on Rehabilitation and Maintenance in Civil Engineering*, *1*, 379–390.

2. Ahmad, S., Rizwan, M., & Khan, A. (2020). Environmental degradation of steel structures in coastal terrains. *Journal of Constructional Steel Research*, *165*, 105892.
3. American Concrete Institute (ACI). (2014a). *Building code requirements for structural concrete and commentary (ACI 318-14)*.
4. American Concrete Institute (ACI). (2014b). *Building code requirements for structural concrete and commentary (ACI 318-14)*. ACI.
5. American Institute of Steel Construction (AISC). (2022). *Specification for structural steel buildings (ANSI/AISC 360-22)*.
6. American Society of Civil Engineers (ASCE). (2017). *Minimum design loads and associated criteria for buildings and other structures (ASCE/SEI 7-16)*.
7. Badan Standardisasi Nasional. (2020a). *Beban minimum untuk perancangan bangunan gedung dan struktur lain (SNI 1727:2020)*.
8. Badan Standardisasi Nasional. (2020b). *Spesifikasi untuk bangunan baja struktural (SNI 1729:2020)*.
9. Belytschko, T., Liu, W. K., Moran, B., & Elkhodary, K. (2014). *Nonlinear finite elements for continua and structures* (2nd ed.). John Wiley & Sons.
10. Birkemoe, P. C. (1996). Behavior of critical steel connections. *Engineering Journal, AISC*, *33*(1), 11–20.
11. Cannon, D. (2019). *Wind load dynamics on open lattice towers and infrastructure*. Springer.
12. Chen, W. F., & Zhao, X. (2021). *Advanced analysis of steel frames*. CRC Press.
13. Cook, R. D., Malkus, D. S., Plesha, M. E., & Witt, R. J. (2007). *Concepts and applications of finite element analysis* (4th ed.). John Wiley & Sons.
14. Efendi, A. W. (2022). Behavior Analysis of Building Structures After a Fire with FEA LISA V. 8. *Kurva S: Jurnal Keilmuan Dan Aplikasi Teknik* …. http://ejurnal.untag-smd.ac.id/index.php/TEKNIKD/article/view/6413
15. Efendi, A. W. (2023). Desain Kandang Sperma Ideal untuk Sapi menggunakan LISA V. 8 FEA. *Jurnal Sintesis: Penelitian Sains, Terapan Dan* …. https://www.jurnal.iik.ac.id/index.php/jurnalsintesis/article/view/71
16. Efendi, A. W. (2024). APPLICATION OF CHATGPT IN THE ANALYSIS OF INTERNAL FORCES OCCURRING IN SIMPLE BEAMS USING LISA V. 8 FEA. *Selodang Mayang: Jurnal Ilmiah Badan* …. https://ojs.selodangmayang.com/index.php/bappeda/article/view/313

17. Efendi, A. W., Do, Y., & Rachman, N. F. (2022). Behavior of Rail Ballast Layer Using Mortar Foam with LISA-FEA. *Journal of Railway Transportation and …*. https://www.jrtt.org/jrtt/article/view/8
18. Efendi, A. W., & Weijia, C. (2023). Buffer stops behavior due to rail impact loads with LISA FEA. *Journal of Railway Transportation and Technology*. https://jrtt.org/jrtt/article/view/20
19. Efendi, A. W., Zulkarnain, A., & Atmaja, D. S. (2022). Behavior of railroad bearing due to temperature and load using LISA FEA. *Journal of Railway Transportation …*. https://mail.jrtt.org/jrtt/article/view/1
20. Eligehausen, R., Mallée, R., & Silva, J. F. (2006). *Anchorage in concrete construction*. Ernst & Sohn.
21. Fukuoka, H. (2017). Mechanics of cable structures and tension systems. *International Journal of Space Structures*, *32*(2), 110–124.
22. Galambos, T. V, & Surovek, A. E. (2008). *Structural stability of steel: Concepts and applications for structural engineers*. John Wiley & Sons.
23. Gere, J. M., & Goodno, B. J. (2012). *Mechanics of materials* (8th ed.). Cengage Learning.
24. Harrington, E. J. (2016). *Mechanical systems for heavy lifting and pulling*. Industrial Press.
25. IDEA StatiCa. (2024). *Theoretical background of CBFEM*.
26. Kulak, G. L., Fisher, J. W., & Struik, J. H. (2001). *Guide to design criteria for bolted and riveted joints* (2nd ed.). American Institute of Steel Construction.
27. Liu, G., Zhang, H., & Wang, T. (2023). Structural innovations in electric vehicle charging infrastructure. *Engineering Structures*, *275*, 115312.
28. MacGregor, J. G., & Wight, J. K. (2005). *Reinforced concrete: Mechanics and design* (4th ed.). Prentice Hall.
29. Machalaba, F. (2018). *Structural design of telecommunication and utility towers*. Routledge.
30. Pasternak, P. L. (1954). *On a new method of analysis of an elastic foundation by means of two foundation constants*. Gosudarstvennoe Izdatelstvo Literatury po Stroitelstvu i Arkhitekture.
31. Putra, A., & Wijaya, I. (2019). Wind environment characteristics in open terrains of Kalimantan. *Procedia Engineering*, *125*, 450–458.
32. Sadovsky, Z. (2015). Asymptotic analysis of wind resistance of steel lattice towers. *Journal of Wind Engineering and Industrial Aerodynamics*, *143*, 120–128.

33. Salmon, C. G., Johnson, J. E., & Malhas, F. A. (2009). *Steel structures: Design and behavior* (5th ed.). Pearson.
34. Sims, U. (2020). *Electric vehicle charging infrastructure: Planning and engineering*. Wiley-Blackwell.
35. Trahair, N. S., Bradford, M. A., & Nethercot, D. A. (2001). *The behavior and design of steel structures to AS4100* (3rd ed.). Spon Press.
36. Wald, F., Sokol, Z., & Steenhuis, M. (2019). *Component-based finite element method for steel joints*. CRC Press.
37. Wang, L., Chen, Y., & Li, X. (2022). Resilience of steel structures under dynamic environmental loads. *Journal of Structural Engineering*, *148*(4), 4022025.
38. Winkler, E. (1867). *Die Lehre von der Elastizität und Festigkeit*. Dominicus.
39. Zienkiewicz, O. C., Taylor, R. L., & Zhu, J. Z. (2013). *The finite element method: Its basis and fundamentals* (7th ed.). Butterworth-Heinemann.